Performance Comparisons of Tunneling Field-Effect Transistors made of InSb, Carbon, and GaSb-InAs Broken Gap Heterostructures

Mathieu Luisier and Gerhard Klimeck
Network for Computational Nanotechnology and Birck Nanotechnology Center,
Purdue University, West Lafayette, IN 47907, USA; email: mluisier@purdue.edu

Abstract

Band-to-band tunneling transistors (TFETs) made of InSb, Carbon, and GaSb-InAs broken gap heterostructures are simulated using an atomistic and full-band quantum transport solver. The performances of two-dimensional single-gate and double-gate devices as well as three-dimensional gate-all-around structures are analyzed and compared to find the most promising TFET design. All transistor types are able to provide a region with a steep subthreshold slope, but despite their low band gap, InSb- and C-based (graphene nanoribbons and carbon nanotubes) devices do not offer high enough ON-currents, contrary to GaSb-InAs broken gap structures. However, the nanoribbon and nanotube TFETs can operate at much lower supply voltages than the III-V transistors.

Introduction

Band-to-band tunneling transistors (TFETs) are very promising devices to help reduce the power consumption of integrated circuits. Due to the tunneling nature of their currents the subthreshold slope (SS) is not limited to 60 mV/dec at room temperature as for MOSFETs. Since the first experimental demonstration of a TFET [1], several groups have successfully fabricated devices capable of breaking the 60 mV/dec limit [2-4]. The common characteristics of these devices are low ON-currents and very short regions with SS below 60 mV/dec.

Physics-based simulations of different TFET types [5-8] predict that these properties can be improved if the device configuration is optimized. It is highly desired to identify early the most appropriate material system(s) for TFETs and to concentrate research in that direction. However, this requires a fair comparison of the various TFET types, which the previous theoretical studies do not provide. They all rely on different simulation approaches like the one-dimensional WKB approximation and ignore the quantization effects that characterize nanoscale devices.

In this paper we use one single tool, an atomistic, quantum mechanical device simulator based on the tight-binding approach to evaluate the performances of lateral p-i-n TFETs with low direct band gaps and the same dimensions. This excludes Si and Ge where phonon-assisted tunneling dominates. Due to their larger band gaps, these materials are not expected to outperform III-V semiconductors. We focus on InSb, Carbon, and GaSb-InAs broken gap devices, with either one-dimensional (nanowires, graphene nanoribbon, and nanotube) or two-dimensional (ultra-thin-body) transport. Pure InAs devices have been treated with our method before and do not seem able to deliver high ON-currents[8]. The unique simulation capabilities that we have developed allow a direct comparison of the performances of these TFETs.

The key findings are that high ON-currents (750 μA/μm) and ON-OFF current ratios ($>$1e7) can be reached, especially in GaSb-InAs structures, but only with a large acceptor doping concentration in the source ($>$1e19 cm^{-3}), an abrupt p-i interface, a supply voltage of at least 0.5 V, and a very good electrostatic control of the channel as in 5nm-thick ultra-thin-body double-gate devices. Graphene nanoribbons, carbon nanotubes, and InSb transistors exhibit too low ON-currents and poorer performances than GaSb-InAs heterostructures. However, Carbon-based TFETs can operate at lower supply voltages (0.2 V) than the III-V semiconductors.

Approach

We have developed a ballistic, multi-dimensional, atomistic, full-band quantum transport simulator dedicated to Si, Ge, III-V ultra-thin-body and nanowire transistors as well as graphene nanoribbon and carbon nanotube devices. Any gate configuration (single, double, all-around) and any transport direction can be simulated. Here, the Schrödinger equation is solved in a nearest-neighbor tight-binding basis (sp^3s^* with spin-orbit coupling for InSb, GaSb, and InAs, p_z orbital model for carbon) using an efficient wave function approach equivalent to the popular NEGF formalism [9], when electron-phonon scattering is not considered, but computationally much more efficient. Carriers are injected from the source and drain contacts into the simulations domain and are either transmitted to the other side of the device or reflected back to their origin. The calculation of the carrier density is self-consistently coupled to that of the Poisson equation solved on a finite element grid.

Results

We consider 9 different p-i-n TFET structures: single- and double-gate ultra-thin-bodies (UTB) as well as gate-all-around nanowires (NW) made of InSb and a GaSb-InAs broken gap (BG) heterostructure (GaSb p-doped source and InAs intrinsic channel and n-doped drain). The 3 other TFETs are single- and double-gate graphene nanoribbons (GNR) and a coaxially gated carbon nanotube (CNT). Some of them are shown in Fig. 1. They all have the same dimensions (5nm of body thickness, diameter, or width, a gate length of 40nm), except the CNT (diameter of 3.4nm giving the same band gap as the

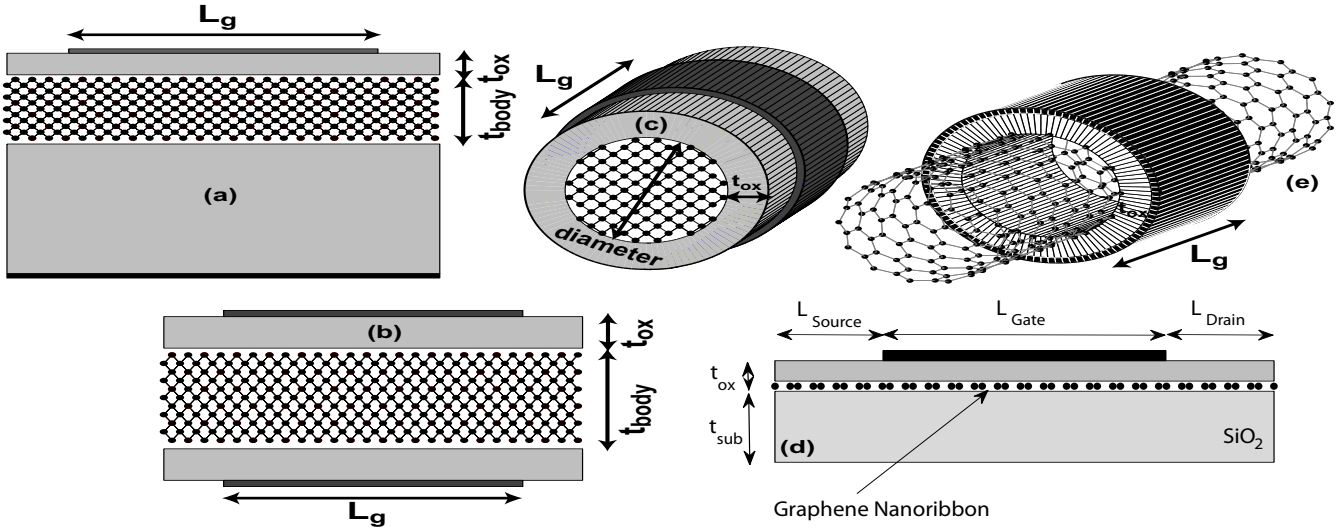

Fig. 1. Schematic view of the different p-i-n tunneling FETs considered in this work. (a) Single-Gate Ultra-Thin-Body (SG UTB), (b) Double-Gate Ultra-Thin-Body (DG UTB), (c) Gate-All-Around Nanowire (GAA NW), (d) Single-Gate Graphene Nanoribbon (SG GNR), and (e) Gate-All-Around Carbon Nanotube (GAA CNT). The UTB and NW are either made of pure InSb or of a relaxed GaSb-InAs heterostructure. In this case, the p-doped region is made of GaSb, the intrinsic channel and the n-doped side of InAs. The body thickness, the diameter, and the ribbon width of all the structures measure 5nm, except the CNT that has a diameter of 3.4nm ($=>$ same band gap as GNR). All the devices are characterized by an EOT of 0.5nm (2nm thick dielectric with ϵ_R=16).

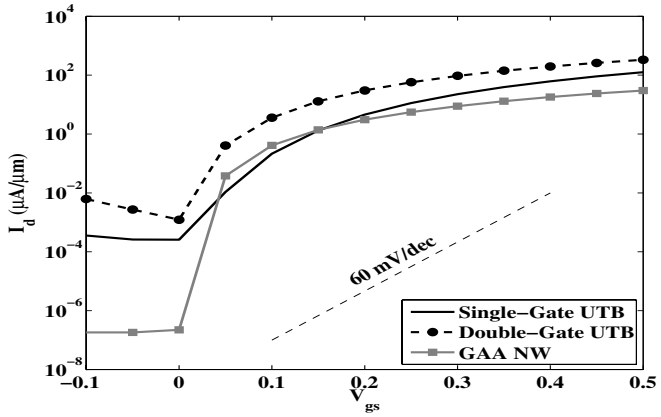

Fig. 2. Transfer characteristics $I_d - V_{gs}$ at V_{ds}=V_{DD}=0.5 V of InSb-based SG UTB (black line), DG UTB (dashed line with circles), and GAA NW (gray line with squares) TFETs. All the devices have a gate length L_g=40nm. The p-doped region measures 30nm and has a doping concentration N_A=4e19 cm^{-3}. The n-doped extension has a length L=120nm and a doping concentration N_D=5e17 cm^{-3}. The nanowire current is normalized by its perimeter.

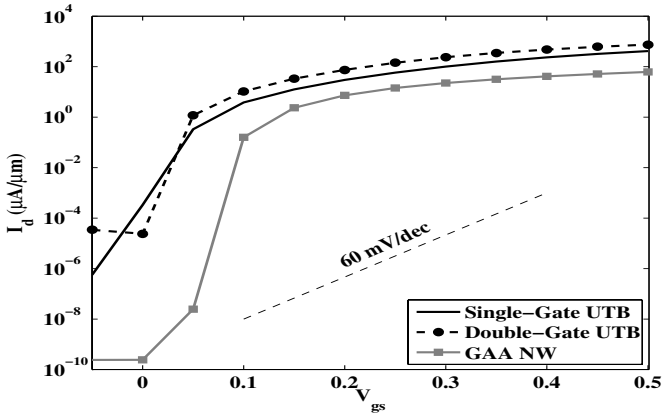

Fig. 3. Same as Fig. 2, but for devices composed of a GaSb-InAs broken gap heterostructure. The supply voltage is V_{DD}=0.5 V. All the TFETs have an InAs gate length L_g=40nm. The GaSb p-doped region measures 20nm and has a doping concentration N_A=4e19 cm^{-3}. The InAs n-doped extension has a length L=80nm and a doping concentration N_D=1e18 cm^{-3}. The nanowire current is normalized by its perimeter.

GNR) and the same EOT of 0.5nm. The p-i and i-n interfaces are abrupt, irrespective of the doping concentration.

The transfer characteristics of the 9 TFETs are shown in Fig. 2 to 4 and the performances are summarized in Table 5. The highest ON-current (750 μA/μm) is obtained for the double-gate GaSb-InAs BG structure which exhibits a OFF-current of 2.4e-5 μA/μm only and a SS of 10.6 mV/dec. To reach these values a high acceptor doping concentration (N_A=4e19 cm^{-3}) and supply voltage (V_{DD}=0.5 V) are required. With the same N_A and V_{DD}, the InSb SG and DG UTBs have 2-3 times smaller ON-current. Carbon-based TFETs have ≈2 times smaller ON-currents, but with a supply voltage of 0.2 V only. The nanowire structures are characterized by lower ON-currents, but an excellent electrostatic control leading to very low SS. Increasing their diameter certainly increases their SS, but also their ON-current. The SS slope of nanowires is expected to remain below 60 mV/dec as long as they operate close to their quantum capacitance limit. It has been already proved that InAs nanowires with a diameter up to at least 10nm operate in this regime [8]. InSb

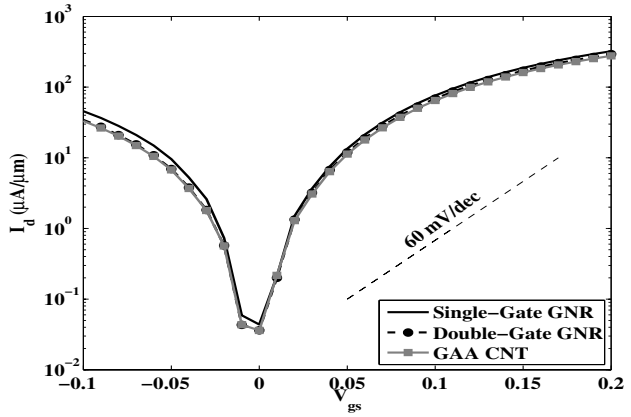

Fig. 4. Same as Fig. 2 and 3, but for carbon-based TFETs with a gate length L_g=40nm. The supply voltage is V_{DD}=0.2 V. The SG and DG graphene nanoribbons as well as the GAA CNT have an average of f=5.5e-4 acceptors per carbon atom in the p-doped side and f=2.2e-4 donors in the n-side.

Device	I_{ON} (μA/μm)	I_{OFF} (μA/μm)	SS (mV/dec)	V_{DD} (V)
SG InSb	125.8	2.56e-4	34.2	0.5
DG InSb	333.1	1.2e-3	19.9	0.5
GAA InSb	29.9	2.2e-7	9.2	0.5
SG BG	418.3	3.32e-4	16.5	0.5
DG BG	752	2.4e-5	10.6	0.5
GAA BG	62	2.4e-10	7.3	0.5
SG GNR	320.4	4.4e-2	13	0.2
DG GNR	291.3	3.6e-2	12.8	0.2
GAA CNT	276.2	3.6e-2	12.9	0.2

Fig. 5. Summary of the tunneling transistor performances from Fig. 2 (InSb devices), 3 (broken gap heterostructures, BG), and 4 (carbon-based TFETs, GNR and CNT). The ON-current (I_{ON}), OFF-current (I_{OFF}), subthreshold slope (SS), and supply voltage (V_{DD}) are given. All the TFETs have a gate length L_g=40nm.

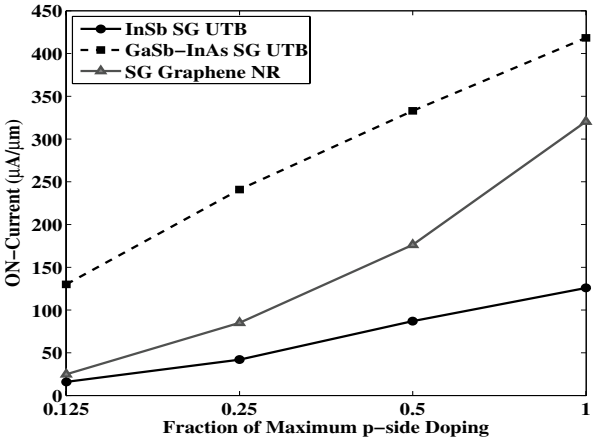

Fig. 6. ON-current (I_d at V_{ds}=V_{gs}=V_{DD}) of the InSb SG UTB (V_{DD}=0.5 V), of the GaSb-InAs heterostructure SG UTB (V_{DD}=0.5 V), and of the SG graphene nanoribbon (V_{DD}=0.2 V) as function of the doping concentration of the p-side. The maximum acceptor concentration is N_A=4e19 cm^{-3} for the III-V devices and f=5.5e-4 doping impurity per carbon atom for the graphene nanoribbon.

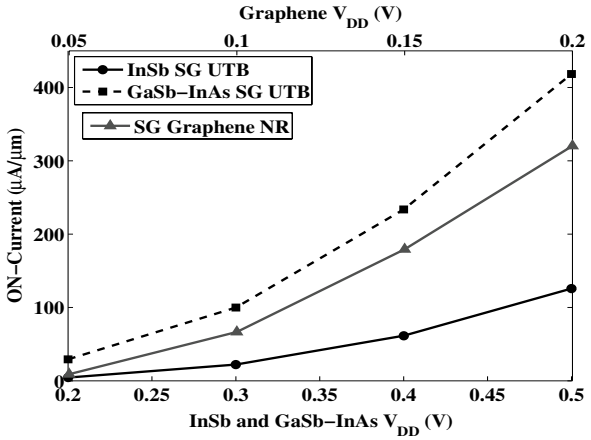

Fig. 7. ON-current (I_d at V_{ds}=V_{gs}=V_{DD}) of the InSb SG UTB, of the GaSb-InAs heterostructure SG UTB, and of the SG graphene nanoribbon as function of the supply voltage V_{DD}. The lower x-axis refers to the III-V devices, the upper to the graphene nanoribbon. The doping concentrations of the p- and n-doped regions remain as in Table 5.

nanowires, due to their lower band gap and electron effective mass, could remain in the quantum capacitance limit up to larger diameters than InAs.

The choice of the p-side doping and of the supply voltage are motivated by the search for high ON-currents as illustrated in Fig. 6 and 7, respectively. The lower donor doping concentration of the drain side is intended to reduce the natural ambipolar behavior of TFETs by increasing the width of the lower tunneling channel as shown in Fig. 8.

The double-gate devices generally have better performances than single-gate ones due to a better electrostatic control resulting in larger electric fields at the source-channel interface and higher tunneling probabilities as depicted in Fig. 9. In GNR the electrostatic control is as good in SG as in DG devices, but the longitudinal fringing fields caused by the gate contact are more important in DG devices.

GaSb-InAs BG TFETs are very sensitive to quantization effects that induce a band gap increase, move the conduction band of InAs above the valence band of GaSb, and reduce the tunneling probability of electrons in the ON-state regime as shown in Fig. 10. However, without this band gap increase the main tunneling channel could not be shut down in the transistor OFF-state. Despite the benefit of energy quantization, the OFF-currents might still be larger than expected due to electron-phonon scattering as sketched in Fig. 11.

Conclusion

We have investigated different structures and materials for potential application as TFETs in low power circuits. III-V

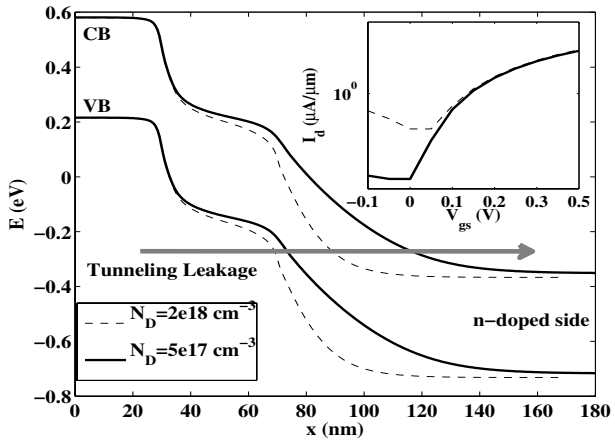

Fig. 8. Band edges of the 5nm thick SG InSb UTB TFET in the OFF-current regime (V_{gs}=0 V, V_{ds}=0.5 V). The n-doped side has either a donor concentration N_D=2e18 cm^{-3} (dashed lines) or N_D=5e17 cm^{-3} (solid lines). The longer depletion region of the lightly doped device reduces the tunneling leakage of the ambipolar channel. The inset shows the corresponding transfer characteristics $I_d - V_{gs}$.

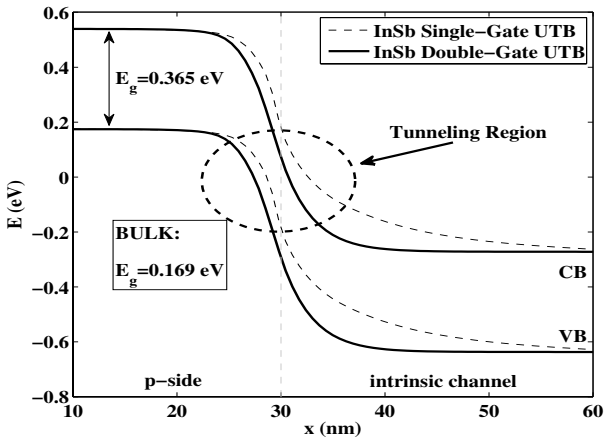

Fig. 9. Band edges of the 5nm tick SG (dashed line) and DG (solid line) InSb UTB TFET at V_{gs}=V_{ds}=0.5 V. The interface region between the heavily doped p-side (N_A=4e19 cm^{-3}) and the intrinsic channel is shown. The better electrostatic control of the DG structure allows a larger tunneling window than for the SG device in the ON-current regime (thinner potential barrier).

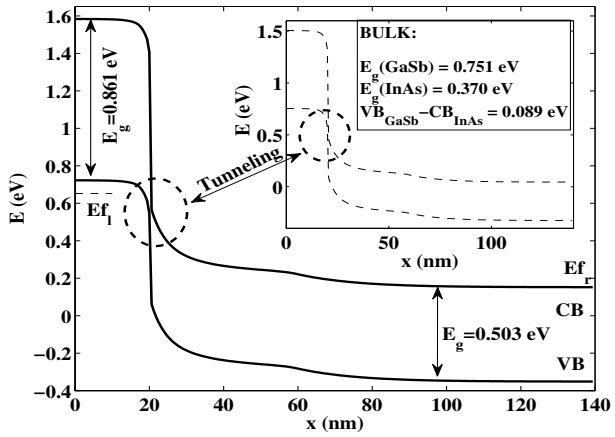

Fig. 10. Band edges of the 5nm thick SG UTB TFET composed of a GaSb-InAs broken gap heterostructure at V_{gs}=V_{ds}=0.5 V. The inset shows the bulk band edges (with the same electrostatic potential). Due to quantization effects, the positive offset of 89 meV between the bulk GaSb valence band and the InAs conduction band vanishes, reducing the tunneling probability of VB electrons.

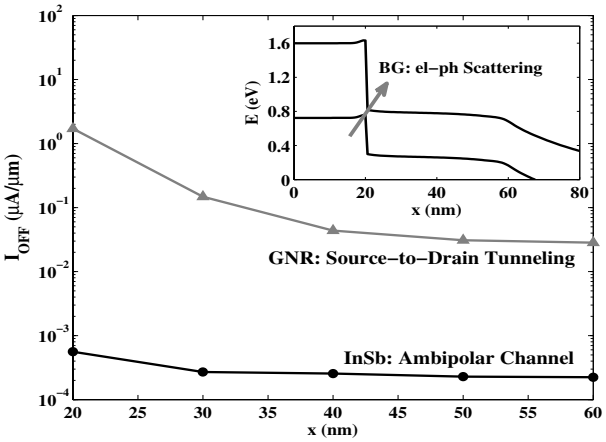

Fig. 11. OFF-current of the the 5nm tick SG InSb UTB (black line with circles) and of the 5nm thick SG graphene NR (gray line with triangles) as function of the channel length. The inset shows that the OFF-current of the GaSb-InAs broken gap heterostructure might be dominated by electron-phonon scattering and cannot be correctly modeled in the ballistic approximation.

broken gap heterostructures appear very promising for their high-ON current, but they require a large doping concentration in the source and a high supply voltage. If low supply voltages are preferred to high ON-currents, graphene nanoribbon might be the ideal candidates. Additional studies including electron-phonon scattering will be conducted to determine the best TFET configuration.

Acknowledgment

This work was partially supported by NSF grant EEC-0228390 that funds the Network for Computational Nanotechnology, by NSF PetaApps grant number 0749140, and by NSF through TeraGrid resources provided by the National Institute of Computational Sciences (NICS).

References

[1] J. Appenzeller et al. Phys. Rev. Lett. 93, 196805, 2004. [2] T. Krishnamohan et al., IEDM Tech. Dig. 2008, p. 947, 2008. [3] W. Y. Choi et al., IEEE Elec. Dev. Lett. 28, p. 743, 2007. [4] K. E. Moselund et al., 67th DRC, p. 23, 2009. [5] C. Hu, 2008 ICSICT, p. 17, 2008. [6], K. K. Bhuwalka et al., Jpn. J. Appl. Phys. 43, p. 4073, 2004. [7] Q. Zhang et al., IEEE Elec. Dev. Lett. 29, p. 1344, 2008. [8] M. Luisier et al., IEEE Elec. Dev. Lett. 30, p. 602, 2009. [9] M. Luisier et al., Phys. Rev. B 74, 205323, 2006.